Am J Transl Res 2022;14(7):4990-5002
www.ajtr.org /ISSN:1943-8141/AJTR0143823

*Original Article*

# Genomic mutation characteristics and prognosis of biliary tract cancer

Lingling Guo[1*], Fuping Zhou[1*], Huiying Liu[1], Xiaoxia Kou[1], Hongjuan Zhang[1], Xiaofeng Chen[2], Jinrong Qiu[1]

[1]*Department of Biological Therapy, Eastern Hepatobiliary Surgery Hospital, Shanghai 201805, China;* [2]*Department of Oncology, Jiangsu Province People's Hospital and Nanjing Medical University First Affiliated Hospital, Nanjing, Jiangsu, China.* [*]*Equal contributors.*

Received April 29, 2022; Accepted June 8, 2022; Epub July 15, 2022; Published July 30, 2022

**Abstract:** Background: The incidence of biliary system cancer is higher in the Chinese population than in the West. The overall prognosis of gallbladder cancer and cholangiocarcinoma is poor, and the current treatment is limited. In order to explore the pathogenesis of biliary tract cancers and potential targeted therapies, we mapped the mutation landscape of biliary tract cancer in the Chinese population and analyzed the molecular mechanism related to prognosis. Methods: A total of 59 formalin fixed paraffin-embedded (FFPE) tissue samples were obtained from patients with operable biliary tract cancer. We conducted targeted capture sequencing of 620 genes through high-throughput sequencing technology and analyzed the fusion information of 13 genes. Results: Mutations were detected in 88% samples, and the most frequent mutation base was C>T. Genes with higher single nucleotide variations (SNV) and copy number variations (CNV) frequency are *TP53*, *KRAS*, *ARID1A*, *VEGFA*, cyclin family related genes and cyclin-dependent kinase genes. Actionable mutations were detected in 59.3% samples, and germline mutations were detected in 22% samples. Patients with *KRAS* mutations, VEGFA pathway mutations and higher tumor mutation burden (TMB) may have poor prognosis. Conclusions: We explored the mutation characteristics and prognostic mechanism of biliary tract cancers in the Chinese population. This study provides potential evidence for targeted therapy and immunotherapy of biliary tract cancers.

**Keywords:** Gene mutation, somatic mutation, germline mutation, mutation landscape, biliary tract cancer, prognosis

## Introduction

Biliary Tract Cancer (BTC) is a malignant tumor originating from the gallbladder and bile duct epithelium, including gallbladder cancer (GBC), intrahepatic cholangiocarcinoma (ICC) and extrahepatic cholangiocarcinoma (ECC). ECC consists of hilar cholangiocarcinoma and distal cholangiocarcinoma [1]. In Western countries, the incidence of cholangiocarcinoma is low, with an annual incidence of 0.35-2 per 100,000 [2]. In Asian countries, the incidence of cholangiocarcinoma is several times higher than that in Western countries. Gallbladder cancer is closely related to cholelithiasis and chronic cholecystitis, accounting for more than 80% of biliary system cancers. The global incidence of gallbladder cancer is 220,000, and the number of deaths is about 165,000 in 2018. In China, the incidence and mortality of gallbladder cancer are 52,800 and 40,700, and the morbidity and mortality are ranked 19th and 12th, respectively [3, 4].

Regardless of location, BTC has potentially high transfer and invasion ability. Due to its anatomical location and distribution along the bile duct, it is difficult to remove completely by surgical resection. Even if it is diagnosed at an early stage, BTC is associated with poor prognosis [5, 6]. Unfortunately, most BTC patients are diagnosed with advanced disease at their first visit and cannot be treated surgically. The 5-year survival rate of these patients is extremely low, about 10% for cholangiocarcinoma and less than 5% for gallbladder cancer [7-9].

There are no molecular markers related to clinical diagnosis, but drugs targeted to IDH1 and FGFR1/2/3 have shown superior performance

**Table 1.** Characteristics of patients with BTC

| Characteristic | Total (n=59) | Any mutation (n=52, 88.1%) | No mutation (n=7, 11.9%) |
|---|---|---|---|
| Age, median | 57.2 (34-75) | 56 | 65 |
| Male gender | 33 | 29 (87.9) | 4 (12.1) |
| Female gender | 26 | 23 (88.5) | 3 (11.5) |
| ECOG | | | |
| 0 | 9 | 8 (88.9) | 1 (11.1) |
| 1 | 26 | 23 (88.5) | 3 (11.5) |
| 2 | 12 | 10 (83.3) | 2 (16.7) |
| Unknown | 12 | 11 (91.7) | 1 (8.3) |
| Cancer type | | | |
| Cholangiocarcinoma | 42 | 37 (88.1) | 5 (11.9) |
| Gallbladder cancer | 17 | 15 (88.2) | 2 (11.8) |
| Stage | | | |
| I | 1 | 1 (100) | 0 (0) |
| II | 7 | 5 (71.4) | 2 (28.6) |
| III | 14 | 12 (85.8) | 2 (14.2) |
| IV | 21 | 21 (100) | 0 (0) |
| Unknown | 16 | 13 (81.3) | 3 (18.7) |

recently [10-12]. The phase III clinical trial ClarIDHy demonstrated IDH1 inhibitor Ivosidenib improved the medium progression free survival (Ivosidenib 2.7 months vs. placebo 1.4 months) of patients with ICC who have been treated by chemotherapy [13]. FGFR2 target drugs such as infigratinib, derazantinib and TAS-120 showed good efficacy and controllable toxicity in phase II study [10-12]. The disease control rate of Infigratinib, a tyrosine kinase inhibitor, as a second-line drug for FGFR2 fusion-positive patients with advanced cholangiocarcinoma was 75.4% [12]. Irreversible pan-FGFR inhibitor, TAS-120, inhibited secondary mutations of FGFR2 and have efficacy in four patients with FGFR2-fusion-positive ICC who developed resistance to BGJ398 or Debio1347 [10]. On April 17th, 2020, the U.S. Food and Drug Administration (FDA) approved pemigatinib for FGFR2 fused cholangiocarcinoma and grants priority review to a variety of FGFR inhibitors for their superior efficacy. The pathogenesis of BTC is still unclear. Several previous studies [14-16] have presented common gene mutation spectrums in BTC in Japanese and western populations. Few studies outline genomic mutation characteristics of such tumors in the Chinese population. The next-generation sequencing with high throughput and high efficiency can perform parallel detection on multiple genes, which has been widely used in recent years. In order to explore the molecular mechanism of BTC and the population that would benefit from targeted therapy, we sequenced 620 genes related to tumorigenesis in 59 BTC samples.

## Materials and methods

### *Clinical samples*

We collected 59 surgical tissue samples of BTC from Eastern Hepatobiliary Surgery Hospital of the Second Military Medical University (Shanghai, China). According to WHO 2015 classification criteria, the tumor samples including 17 cases of gallbladder cancer and 42 cases of cholangiocarcinoma. All tissue samples were paired with blood samples to rule out nonpathogenic germline mutations. Follow-up data of 26 samples were obtained from Eastern Hepatobiliary Surgery Hospital of the Second Military Medical University. The clinical features included sex, age, tumor location, TNM stage, ECOG score and other information that are presented in **Table 1**. All the patients in our study signed an informed consent.

### *Library building and sequencing*

DNA was extracted from FFPE-fixed tumor tissue or peripheral blood using QIAamp DNA FFPE Tissue Kit (Qiagen). NimbleGen SeqCap EZ choice capture panel was used to capture the coding region of 620 genes (Supplementary Table 1) and the splicing sites. The DNA libraries were built according to the procedure of KAPA Hyper Prep protocols (KAPA). The final libraries were sequenced on the Illumina Novoseq6000 (PE150) sequencer, and the original FASTQ file was obtained. The final libraries were sequenced by Illumina Novoseq6000 (PE150).

### *SNV and indel calling*

Trimmomatic was used to filter the sequenced FASTQ files, and Burrows-Wheeler Aligner (BWA) was used to align the reads with the reference genome GRCh37 (hg19). Duplicates generated by PCR were removed by SAMtools.

SNVs were called by Mutect2 with a paired workflow. ANNOVAR was used to annotate the variants. We filtered the obtained SNVs according to the following conditions: (1) base quality value ≥20; (2) mutation reads depth ≥4; (3) variant allele frequency ≥1%; (4) reads supporting variation <4 in normal, tumor abundance/normal abundance ≥8; (5) no strand bias (GATK parameter FS >60 for SNP and FS >200 for indel); (6) discard synonymous mutations; (7) variation not in the dbSNP database.

*Copy number variation (CNV) analysis*

When the dispersion is normal, we set the cut-off values for CNV as 1.5 and 0.5 copies. It is regarded as copy number amplification when the value is larger than 1.5, and it is regarded as copy number deletion when the value is smaller than 0.5.

*TMB calculating*

TMB is defined as the number of SNV mutations per megabase. We kept mutations with mutation frequency ≥5% and removed synonymous mutations.

*Driver mutation analysis*

Driver genes were identified using oncodriveCLUST software, which is based on mutation frequency. The loss-of-function (LoF) gene mutations in the coding region were used as background. Gain-of-function (GoF) gene mutations were analyzed as key points.

*Germline variant calling*

Filter germline variants were obtained by GATK according to the following conditions: (1) mutation depth ≥50; (2) variation frequency ≥30%; (3) discard synonymous mutations; (4) population frequency ≤1/1,000 in ExAC, 1,000 genome and other database; (5) according to the ClinVar database, we reserved the splicing, stop-gain, frameshift, or (likely) pathogenic variants.

*Survival analysis*

All the analysis and graphs were based on R software. The survfit and survdiff functions in R were used to generate Kaplan-Meier survival curves and calculate the *P* value of the log-Rank test. Genes with more than 4 mutations were included in the survival analysis.

## Results

*Mutation signature*

Target capture sequencing was conducted in all 59 BTC samples, with an average sequencing depth of 2,500X. At least one mutation was detected in 88% of tumor samples. In total, we identified 853 somatic mutations, including 736 SNVs and 99 indels. Among all the mutations, there were 649 missense, 77 nonsense, 78 frameshift, and 7 splicing mutations. The overall SNV mutation rate was 55.66 muts/Mb, and the Indel mutation rate was 7.49 muts/Mb. The mutation rates of cholangiocarcinoma and gallbladder cancer were 30.25 muts/Mb and 25.41 muts/Mb, respectively. In this study, C>T was found to be the most common type of mutation, accounting for 62.4% of all SNVs (**Figure 1A**). Non-negative matrix factorization (NMF) was used to identify mutant signatures of BTC. This analysis identified two different signatures: signature A is characterized by (A/C/T/G) CG> (A/C/T/G) TG, and signature B is characterized by TC (A/C/T) <TG (A/C/T) and TC (A/T/C/G) <TT (A/T/C/G) (**Figure 1A**). We compared the identified signature with the COSMIC signature and found that signature A is similar to COSMIC signature SBS1 and SBS6 (cosine similarity is 0.66 and 0.68 respectively), and that signature B is similar to COSMIC SBS13 (cosine similarity is 0.78) (**Figure 1B**).

We profiled the somatic mutation maps of BTC (**Figure 2A**). A total of 603 genes were mutated in all BTC samples, and most of the gene mutations appeared at least in one sample. We found 47% of all 59 patients harbored the TP53 mutation, significantly higher than previously reported (33%, 26%) [15, 16]. The mutation frequencies of TP53 in cholangiocarcinoma and gallbladder cancer were 43% and 80%, respectively (**Figure 2B**, **2C**), and both are higher than previously reported. TP53 gene mutations had no hot spot, but were mainly in the DNA binding domain (**Figure 3**). In previous reports, KRAS, with mutation frequency ranging from 5% to 18%, was the gene with the second most significant number of mutations after TP53 [15-17]. In this study, the KRAS mutation frequency was 19%, and the frequencies in cholangiocarcinoma and gallbladder cancer were 24% and 13%, respectively (**Figure 2B**, **2C**). We used oncodriverCLUST to analyze the possible driver genes and found that KRAS and IDH1 muta-

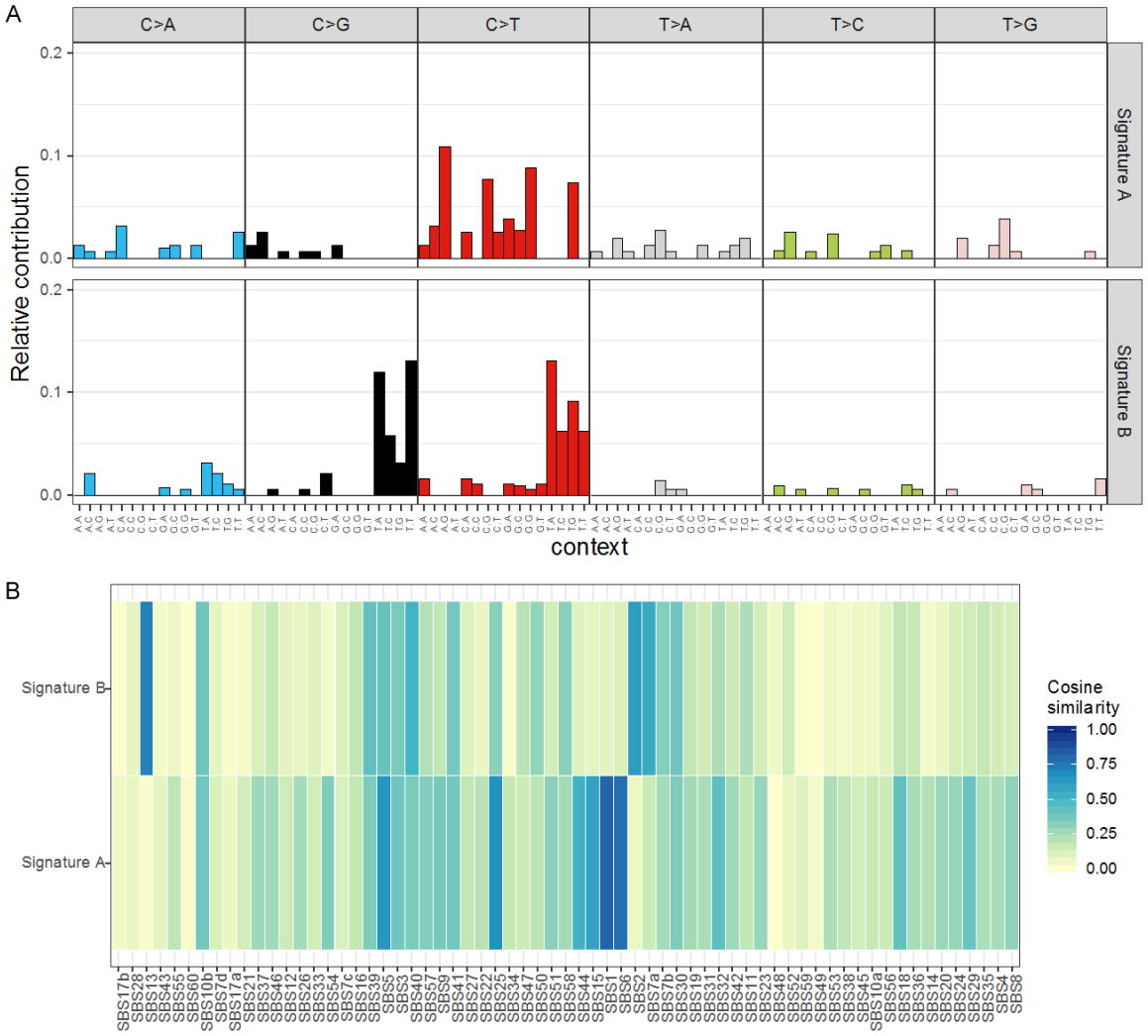


**Figure 1.** Mutational signatures. A. Mutational signatures identified in BTC. Two mutational signatures were detected in 59 patients' tumor samples with BTC. B. Identified signatures compared to the COSMIC signatures. The two mutational signatures detected in the 59 BTC samples were compared with the corresponding COSMIC signatures determined by cosine similarity: signature A is similar to SBS1 (cosine similarity =0.66) and SBS6 (cosine similarity =0.68); signature B is similar to SBS13 (cosine similarity =0.78).

tions were driver mutations (Supplementary Table 3).

In addition to the above genes, other frequently mutated genes in this study included ARID1A, KMT2C, ATM, BRCA2, PBRM1, SMARCA4 et al. We estimated that ARID1A was mutated in 17% of all patients in this study, slightly higher than that was recorded in the COSMIC database (12%). The proteins encoded by the ARID1A, ARID1B, PBRM1 and ARID2 genes are all parts of the large ATP-dependent chromatin remodeling complex SNF/SWI. ARID1A is the largest subunit in the SWI/SNF chromatin remodeling complex, which has activities of helicase and ATPase, and regulates transcription by changing the chromatin structure of specific genes [18].

*Copy number variation (CNV)*

CNV is one of the driver factors of carcinogenesis and can directly affect gene transcription and protein expression. In this study, CNV was calculated based on the relative coverage of tumor samples and normal samples. We used GISTIC2.0 to analyze statistically significant local amplifications or deletions, and found that CNV occurred in 35.6% of patient samples (**Figure 4A**). Frequently amplified or deleted

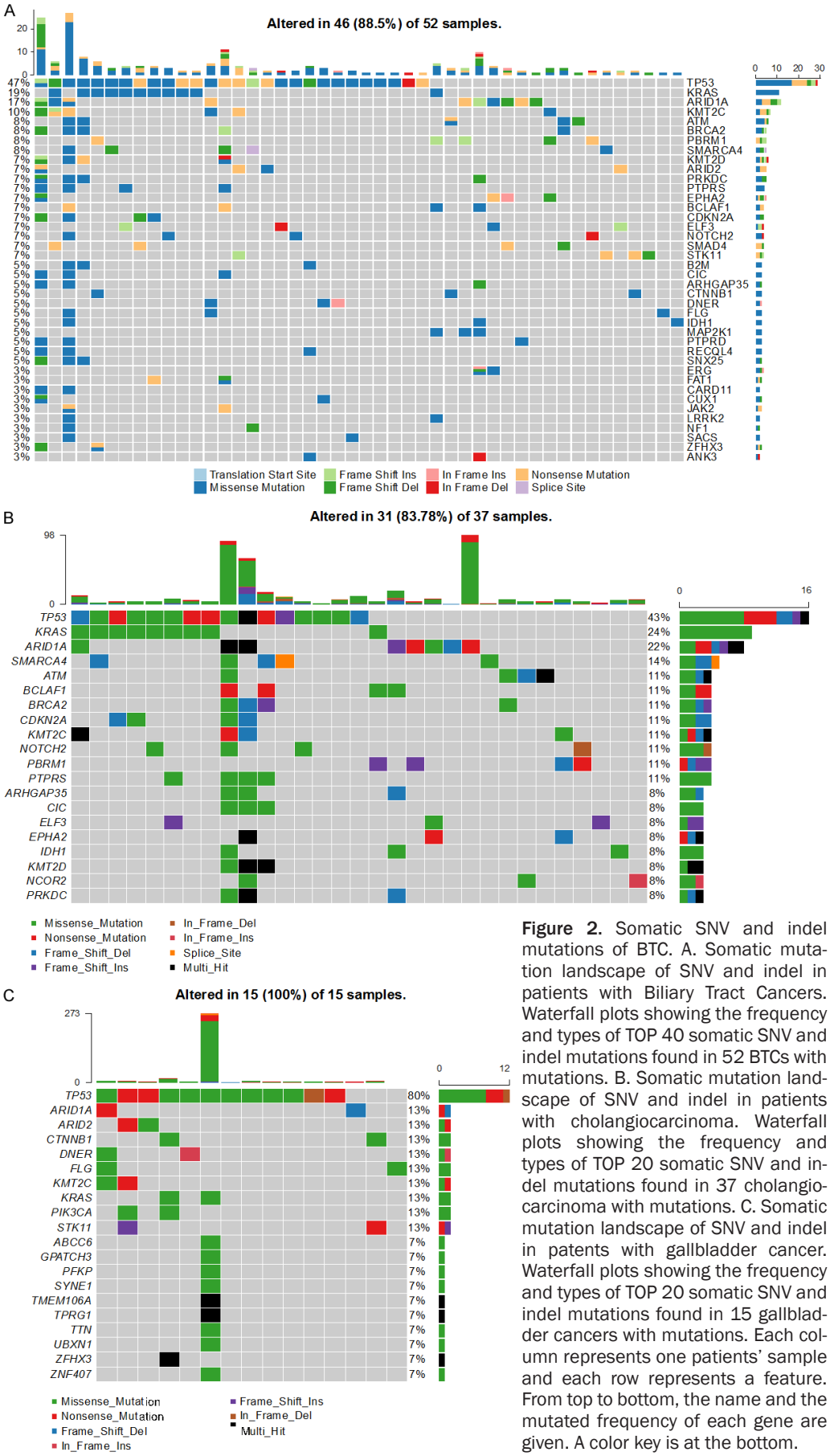


**Figure 2.** Somatic SNV and indel mutations of BTC. A. Somatic mutation landscape of SNV and indel in patients with Biliary Tract Cancers. Waterfall plots showing the frequency and types of TOP 40 somatic SNV and indel mutations found in 52 BTCs with mutations. B. Somatic mutation landscape of SNV and indel in patients with cholangiocarcinoma. Waterfall plots showing the frequency and types of TOP 20 somatic SNV and indel mutations found in 37 cholangiocarcinoma with mutations. C. Somatic mutation landscape of SNV and indel in patents with gallbladder cancer. Waterfall plots showing the frequency and types of TOP 20 somatic SNV and indel mutations found in 15 gallbladder cancers with mutations. Each column represents one patients' sample and each row represents a feature. From top to bottom, the name and the mutated frequency of each gene are given. A color key is at the bottom.

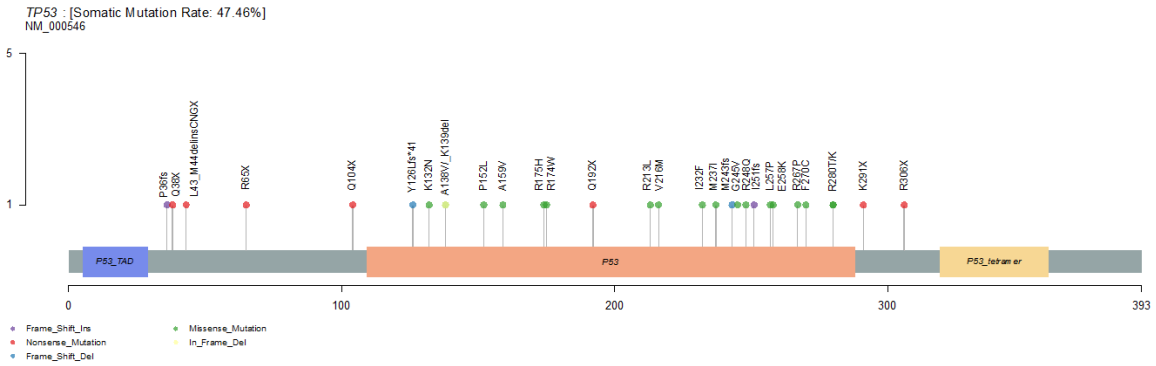


**Figure 3.** Mutation sites of TP53. Distribution of spot mutations on full length TP53 gene with a bar code representing their frequency was presented. Twenty-eight of 59 BTC patients' samples were identified with TP53 mutated spots. No hot spot was found, and mutations were mainly in the DNA binding domains. A color key is at the bottom.

genes included vascular endothelial growth factor A encoding gene VEGFA, cyclin family genes (CCND1, CCND2, CCND3), cyclin dependent kinase genes (CDK12, CDK6), cyclin dependent kinase inhibition genes (CDKN2A, CDKN2B), Erb-B2 receptor tyrosine kinase encoding gene ERBB2 and other genes such as MYC, MDM4, MDM2.

Statistical analysis showed that the chromosome segments that are more prone to amplification and deletion were 6p21.1 and 5q35.3, respectively (**Figure 4B**). The 6p21.1 region occurs in a variety of cancer types in Chinese population, including lung cancer and esophageal cancer, and is also associated with various familial genetic diseases such as hypertension and atherosclerosis [19]. CNV in the 5q35.3 region is relatively rare and has been reported in pancreatic cancer [20].

*Pathway enrichment analysis*

In order to explore the molecular mechanism of BTC, KEGG pathway enrichment analysis was used to enrich somatic mutant genes into important signaling pathways. Among these pathways, the tumor associated signal pathways with frequent gene mutations are PI3K-Akt, MAPK and Ras signaling pathways (**Figure 5**). PI3K-AKT signaling pathway (Supplementary Figure 1A) not only regulates tumor cell proliferation, but also is closely related to tumor angiogenesis [21]. The Ras-Raf-MAPK signal transduction pathway (Supplementary Figure 1B) is involved in the signal transduction of various activated growth factors, cytokines, mitogens and hormone receptors, and plays an important role in regulating cell proliferation, growth and differentiation. Mitogen activated protein kinase (MAPK) can promote vascular endothelial cell proliferation and neovascularization, which can provide more nutrients for tumors, accelerate tumor growth, and promote the spread of cancer cells [22].

*Germline variants in BTC patients*

In order to explore the genetic characteristics of cancer in the biliary system, we analyzed germline mutations in 61 genes (Supplementary Table 2) associated with genetic susceptibility. Germline mutations in BTC have been reported in several studies, and the reported detection frequency is 10%-20% [23]. Germline mutations were found in 13 (22%) patients' samples in this study. Each germline mutation was detected in only one patient sample, and most of them were truncated, frameshift or splicing variations with high evidence of pathogenicity. Germline mutations are mostly DNA damage repair related genes, such as Lynch syndrome related mismatch repair genes MLH3, MSH6 [24, 25], nucleotide excision repair gene ERCC4, DNA single-strand damage repair gene XRCC1. Germline mutations have also occurred in other genes including POLD1, XRCC1, IKZF1, ERCC4, TLR4, EPPK1, CDKN1A, NCOA3 and FGFR1. So far all these mutation nucleotide sites above have not been reported in biliary tract cancers (**Table 2**).

*Survival impacts of molecular characteristics*

To analyze the relationship between molecular characteristics and prognosis, we obtained sur-

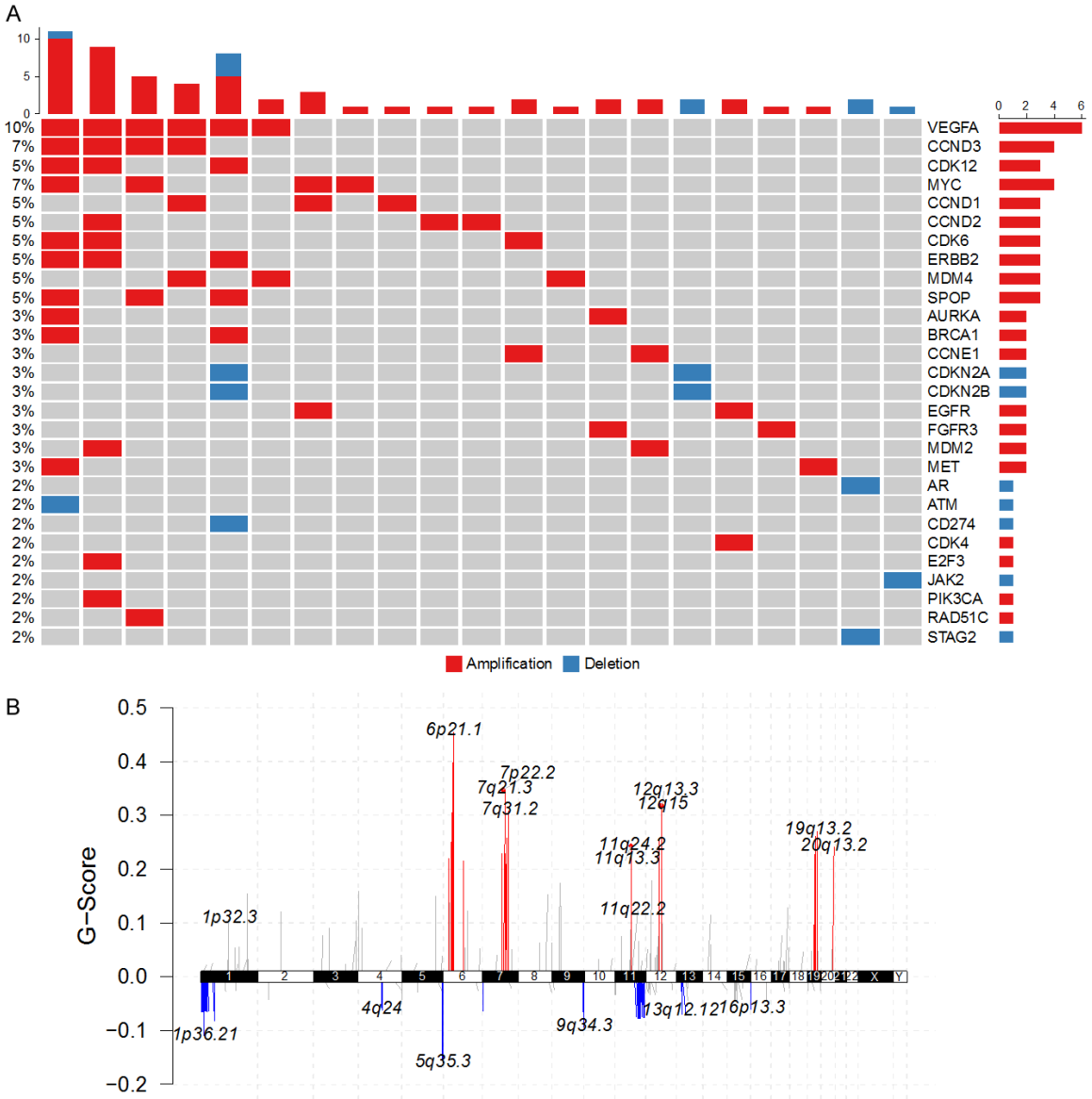


**Figure 4.** Somatic copy number variation (CNV) spectrum of BTC. A. Waterfall plots showing the frequency and types of the TOP 28 somatic CNV found in BTC. Each column represents one of the 59 BTC samples and each row represents a feature. From top to bottom, the name and the mutated frequency of each gene are given. A color key is at the bottom. B. CNVs concentration region of 59 BTC patients on the chromosome.

vival information of 26 patients and plotted Kaplan-Meier survival curves by univariate analysis. Patients with KRAS mutations had worse median overall survival (OS, 108 d vs. 320.5 d, p=0.00057) (**Figure 6A**) among all patients in this study. We also compared the effects of mutations in various signaling pathways on survival and found that gene mutations in the VEGFR signal pathway had a significantly negative impact on OS (144.5 d vs. 324.5 d, p=0.0077) (**Figure 6B**). In addition, we analyzed the correlation between TMB and survival in stage IV patients. Patients whose TMB was higher than the median TMB had worse prognosis than those below (172.5 d vs. 474 d, p=0.05) (**Figure 6C**).

## Discussion

We identified some molecular characteristics of biliary tract cancers through targeted capture sequencing. Among all the mutated bases, C>T bases accounted for the largest proportion, which is consistent with previous reports

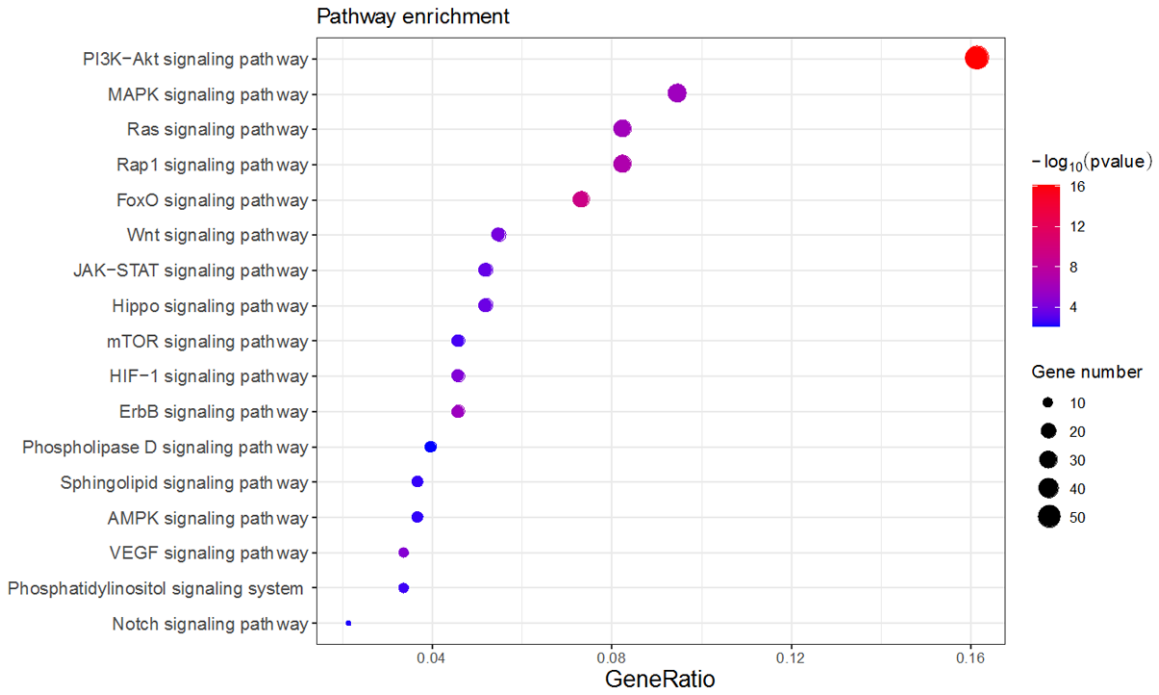


**Figure 5.** Signal transduction pathway enrichment. Kyoto Encyclopedia of Genes and Genomes (KEGG) analyses were conducted using the clusterProfiler package of R software. *P* value <0.05 was set as the cutoff criterion. The tumor associated signal pathways with frequent gene mutations are PI3K-Akt, MAPK, and Ras signaling pathways.

[15-17]. The mutation signatures were similar to COSMIC signature SBS1, SBS6 and SBS13. Signature SBS1 is an endogenous mutation process, triggered by spontaneous or enzymatic deamination of 5-methylcytosine to thymine, resulting in G:T mismatch in double-stranded DNA. Failure to detect and eliminate these mismatches before DNA replication always causes C to replace T. Signature SBS6 is associated with DNA mismatch repair deficiency, and often occurs in microsatellite unstable tumors. SBS13 is related to the cytosine deaminase activity of the AID/APOBEC family which may be caused by the replication of the basic site generated by the error-prone polymerase (such as REV1) during base excision and repair of uracil [26]. Series of DNA damage and repair deficiency may be the internal cause of biliary tract cancers.

TP53 encodes a tumor suppressor protein which contains transcriptional activation, DNA binding and oligomeric domains. The protein encoded by TP53 responds to various cell pressures, regulates target gene expression, and thereby induces cell cycle arrest, apoptosis, aging, DNA repair or metabolic changes. TP53 mutations are ubiquitous in many cancer types, most of which are frameshift or nonsense mutations that lead to protein inactivation. These mutations are widely distributed throughout the whole gene, and occur most frequently in the DNA binding domain [27, 28]. KRAS mutation is a key driver of oncogenesis [29]. We also found that frequently mutation of KRAS might be the driver mutation of BTC. Ongoing cancer driver gene discovery efforts have identified many new drivers within the RAS pathway [30, 31]. In addition, there are already preliminary results of clinical trials, and AMG510 targeting KRAS G12C is particularly prominent [32]. It has opened a historic gap and helped patients with KRAS mutation. Adagrassib (mrtx849) has excellent clinical data recently [33]. Genes encoding SWI/SNF chromatin remodeling complexes such as ARID1A, ARID1B, PBRM1 and ARID2 were also frequently mutated in this study. Recent studies have found that ARID1A mutation is associated with microsatellite instability, C>T mutation pattern, and increased mutational burden in many kinds of tumors. Those tumors formed by ARID1A-deficient ovarian cancer cell lines in mice have increased mutations, more tumor-

**Table 2.** Germline gene mutations

| Patient ID | Cancer Type | Gene | Chrom | Start_Position | End_Position | Nucleotide change | Protein change | Location | Variant classification |
|---|---|---|---|---|---|---|---|---|---|
| 1810276 | cholangiocarcinoma | IKZF1 | chr7 | 50459525 | 50459525 | c.688G>A | p.A230T | exon6 | Missense |
| 1810285 | gallbladder carcinoma | TLR4 | chr9 | 120476505 | 120476505 | c.2099dupT | p.P701fs | exon3 | Frame_Shift_Ins |
| 1810285 | gallbladder carcinoma | POLD1 | chr19 | 50912119 | 50912119 | c.1853dupA | p.Y618_T619delinsX | exon15 | Nonsense |
| 1810455 | cholangiocarcinoma | EPPK1 | chr8 | 144947313 | 144947313 | c.108dupC | p.R37fs | exon2 | Frame_Shift_Ins |
| 1810558 | gallbladder carcinoma | RFWD2 | chr1 | 176054978 | 176054978 | c.1075C>T | p.R359X | exon10 | Nonsense |
| 1830007 | gallbladder carcinoma | XRCC1 | chr19 | 44079097 | 44079097 | c.109A>T | p.K37X | exon2 | Nonsense |
| 1830027 | cholangiocarcinoma | CDKN1A | chr6 | 36652317 | 36652317 | c.439A>G | p.M147V | exon2 | Missense |
| 1910201 | cholangiocarcinoma | NCOA3 | chr20 | 46279949 | 46279949 | c.3875T>C | p.M1292T | exon20 | Missense |
| 1910783 | cholangiocarcinoma | FGFR1 | chr8 | 38271190 | 38271190 | c.2518C>T | p.R840X | exon19 | Nonsense_Mutation |
| 1912566 | cholangiocarcinoma | ERCC4 | chr16 | 14026143 | 14026143 | c.1102+1G>A | . | intron6/7 | Splice_Site |
| 1912694 | cholangiocarcinoma | INSRR | chr1 | 156816322 | 156816322 | c.1798dupA | p.T600fs | exon8 | Frame_Shift_Ins |
| 1912695 | cholangiocarcinoma | TRAF3 | chr14 | 103342048 | 103342048 | c.385A>G | p.M129V | exon4 | Translation_Start_Site |
| 1930095 | cholangiocarcinoma | MLH3 | chr14 | 75513610 | 75513610 | c.2749C>T | p.Q917X | exon2 | Nonsense |
| 1930184 | cholangiocarcinoma | MSH6 | chr2 | 48033987 | 48033987 | c.4068_4071dupGATT | p.K1358fs | exon10 | Frame_Shift_Ins |

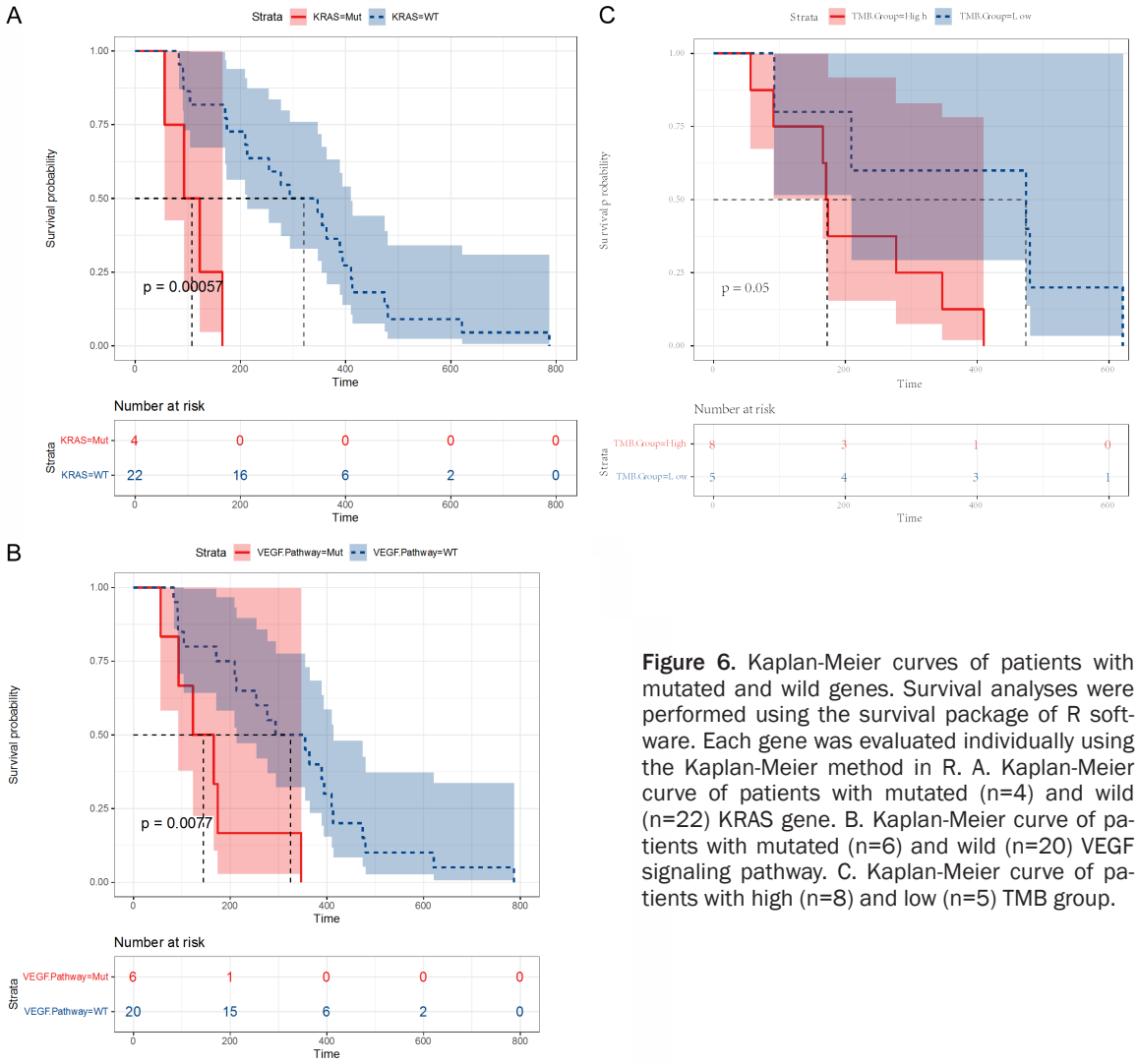


**Figure 6.** Kaplan-Meier curves of patients with mutated and wild genes. Survival analyses were performed using the survival package of R software. Each gene was evaluated individually using the Kaplan-Meier method in R. A. Kaplan-Meier curve of patients with mutated (n=4) and wild (n=22) KRAS gene. B. Kaplan-Meier curve of patients with mutated (n=6) and wild (n=20) VEGF signaling pathway. C. Kaplan-Meier curve of patients with high (n=8) and low (n=5) TMB group.

infiltrating lymphocytes and PD-L1 expression. PD-L1 monoclonal antibodies can reduce tumor burden and prolong survival of mice, but it cannot inhibit ARID1A wild-type ovarian tumors. ARID1A deficiency may lead to tumor MMR deficiency, and patients with ARID1A deficiency may benefit from immune checkpoint inhibitors [34].

Genes encoding vascular endothelial growth factor A (VEGFA), cyclin family, cyclin-dependent kinase, cyclin-dependent kinase inhibitor and others had higher frequency of CNV than others. The protein encoded by VEGFA belongs to the PDGF/VEGF family whose products play an important role in angiogenesis and endothelial cell growth. The expression of VEGFA is upregulated in various tumors including cholangiocarcinoma, which can induce endothelial cell proliferation, promote tumor cell migration and inhibit apoptosis [35-37]. Given the importance of CCND and CDK, the development of CDK4/CDK6 inhibitors has been a strategy for the generation of new anticancer drugs [38, 39].

In this study, the incidence of germline mutations was 22%, slightly higher than previously reported [23]. Germline mutations of DDR genes are associated with increased mutation load, which causes patients with these mutations to possibly be more sensitive to PARP inhibitors and platinum-based treatments. Germline mutations may be a susceptible factor for the occurrence of BTC. Screening for germline mutations in susceptible people is of great importance in prevention and treatment of biliary tract cancers.

Patients with KRAS mutations and VEGF signaling pathway mutations have shorter overall survival. As a cancer-driven event, KRAS mutation is a predictor of drug resistance and poor prognosis for various cancers [29]. Abnormal VEGF signaling pathway promotes tumor cell proliferation and migration, often leading to poor prognosis [40, 41]. In addition, TMB-H patients also exhibited poor OS in this study, possibly due to complicated tumor clone composition and carcinogenesis mechanism. In clinical practice, patients with poor prognosis are suggested to adopt more aggressive treatment and rigorous and regular follow up. Patients with high TMB may be eligible for immunotherapy such as PD-1/PD-L1 inhibitors.

According to the classification of oncoKB, the proportion of actionable gene mutations in the study was up to 59.3% (Supplementary Table 4). As more therapeutic targets are in research and more targeted drugs are being approved, there are more opportunities for biliary tract cancer patients with actionable gene mutations to receive precision medicine in the future. With the rapid development of the next-generation genome sequencing technology, defining of somatic or germline mutation in BTC patients could help accurately identify patients benefiting from drugs such as PARP inhibitors and immune checkpoint inhibitors.

The limited number of samples, insufficient clinical information and not using the whole exon sequencing may be deficiencies of this study. In later research, it is necessary to expand the research cohort with comprehensive clinical information and analyze samples with the whole exon sequencing and other necessary methods. Future prospective research is needed to verify the correlation between specific molecular characteristics and prognosis.

## Acknowledgements

We acknowledge the work of geneticists involved in the analysis of the gene mutations of samples in this study (Zhiyong Li, Ning He, Panpan Song).

## Disclosure of conflict of interest

None.

**Address correspondence to:** Jinrong Qiu, Department of Biological Therapy, Eastern Hepatobiliary Surgery Hospital, No. 700, North Moyu Road, Jiading District, Shanghai 201805, China. Tel: +86-18001657788; E-mail: jrqiu@njmu.edu.cn; Xiaofeng Chen, Department of Oncology, Jiangsu Province People's Hospital and Nanjing Medical University First Affiliated Hospital, No. 300, Guangzhou Road, Gulou District, Nanjing, Jiangsu, China. Tel: +86-13585172066; E-mail: chenxiaofengnjmu@163.com

## References

[1] Banales JM, Cardinale V, Carpino G, Marzioni M, Andersen JB, Invernizzi P, Lind GE, Folseraas T, Forbes SJ, Fouassier L, Geier A, Calvisi DF, Mertens JC, Trauner M, Benedetti A, Maroni L, Vaquero J, Macias RI, Raggi C, Perugorria MJ, Gaudio E, Boberg KM, Marin JJ and Alvaro D. Expert consensus document: cholangiocarcinoma: current knowledge and future perspectives consensus statement from the European Network for the Study of Cholangiocarcinoma (ENS-CCA). Nat Rev Gastroenterol Hepatol 2016; 13: 261-280.

[2] Bridgewater JA, Goodman KA, Kalyan A and Mulcahy MF. Biliary tract cancer: epidemiology, radiotherapy, and molecular profiling. Am Soc Clin Oncol Educ Book 2016; 35: e194-203.

[3] Chen W, Zheng R, Baade PD, Zhang S, Zeng H, Bray F, Jemal A, Yu XQ and He J. Cancer statistics in China, 2015. CA Cancer J Clin 2016; 66: 115-132.

[4] Bray F, Ferlay J, Soerjomataram I, Siegel RL, Torre LA and Jemal A. Global cancer statistics 2018: GLOBOCAN estimates of incidence and mortality worldwide for 36 cancers in 185 countries. CA Cancer J Clin 2018; 68: 394-424.

[5] Jarnagin WR, Fong Y, DeMatteo RP, Gonen M, Burke EC, Bodniewicz BS J, Youssef BA M, Klimstra D and Blumgart LH. Staging, resectability, and outcome in 225 patients with hilar cholangiocarcinoma. Ann Surg 2001; 234: 507-517; discussion 517-519.

[6] Roa I, Ibacache G, Munoz S and de Aretxabala X. Gallbladder cancer in Chile: pathologic characteristics of survival and prognostic factors: analysis of 1,366 cases. Am J Clin Pathol 2014; 141: 675-682.

[7] Razumilava N and Gores GJ. Cholangiocarcinoma. Lancet 2014; 383: 2168-2179.

[8] Hundal R and Shaffer EA. Gallbladder cancer: epidemiology and outcome. Clin Epidemiol 2014; 6: 99-109.

[9] Wakai T, Shirai Y, Moroda T, Yokoyama N and Hatakeyama K. Impact of ductal resection margin status on long-term survival in patients undergoing resection for extrahepatic cholangiocarcinoma. Cancer 2005; 103: 1210-1216.

[10] Goyal L, Shi L, Liu LY, Fece de la Cruz F, Lennerz JK, Raghavan S, Leschiner I, Elagina L, Sir-

avegna G, Ng RWS, Vu P, Patra KC, Saha SK, Uppot RN, Arellano R, Reyes S, Sagara T, Otsuki S, Nadres B, Shahzade HA, Dey-Guha I, Fetter IJ, Baiev I, Van Seventer EE, Murphy JE, Ferrone CR, Tanabe KK, Deshpande V, Harding JJ, Yaeger R, Kelley RK, Bardelli A, Iafrate AJ, Hahn WC, Benes CH, Ting DT, Hirai H, Getz G, Juric D, Zhu AX, Corcoran RB and Bardeesy N. TAS-120 overcomes resistance to ATP-competitive FGFR inhibitors in patients with FGFR2 fusion-positive intrahepatic cholangiocarcinoma. Cancer Discov 2019; 9: 1064-1079.

[11] Mazzaferro V, El-Rayes BF, Droz Dit Busset M, Cotsoglou C, Harris WP, Damjanov N, Masi G, Rimassa L, Personeni N, Braiteh F, Zagonel V, Papadopoulos KP, Hall T, Wang Y, Schwartz B, Kazakin J, Bhoori S, de Braud F and Shaib WL. Derazantinib (ARQ 087) in advanced or inoperable FGFR2 gene fusion-positive intrahepatic cholangiocarcinoma. Br J Cancer 2019; 120: 165-171.

[12] Javle M, Lowery M, Shroff RT, Weiss KH, Springfeld C, Borad MJ, Ramanathan RK, Goyal L, Sadeghi S, Macarulla T, El-Khoueiry A, Kelley RK, Borbath I, Choo SP, Oh DY, Philip PA, Chen LT, Reungwetwattana T, Van Cutsem E, Yeh KH, Ciombor K, Finn RS, Patel A, Sen S, Porter D, Isaacs R, Zhu AX, Abou-Alfa GK and Bekaii-Saab T. Phase II study of BGJ398 in patients with FGFR-altered advanced cholangiocarcinoma. J Clin Oncol 2018; 36: 276-282.

[13] Abou-Alfa GK, Macarulla Mercade T, Javle M, Kelley RK, Lubner S, Adeva J, Cleary JM, Catenacci DV, Borad MJ, Bridgewater JA, Harris WP, Murphy AG, Oh DY, Whisenant J, Wu B, Jiang L, Gliser C, Pandya SS, Valle JW and Zhu AX. LBA10_PR - ClarIDHy: a global, phase III, randomized, double-blind study of ivosidenib (IVO) vs. placebo in patients with advanced cholangiocarcinoma (CC) with an isocitrate dehydrogenase 1 (IDH1) mutation. Ann Oncol 2019; 30: v872-v873.

[14] Maynard H, Stadler ZK, Berger MF, Solit DB, Ly M, Lowery MA, Mandelker D, Zhang L, Jordan E, El Dika I, Kemel Y, Ladanyi M, Robson ME, O'Reilly EM and Abou-Alfa GK. Germline alterations in patients with biliary tract cancers: a spectrum of significant and previously underappreciated findings. Cancer 2020; 126: 1995-2002.

[15] Nakamura H, Arai Y, Totoki Y, Shirota T, Elzawahry A, Kato M, Hama N, Hosoda F, Urushidate T, Ohashi S, Hiraoka N, Ojima H, Shimada K, Okusaka T, Kosuge T, Miyagawa S and Shibata T. Genomic spectra of biliary tract cancer. Nat Genet 2015; 47: 1003-1010.

[16] Wardell CP, Fujita M, Yamada T, Simbolo M, Fassan M, Karlic R, Polak P, Kim J, Hatanaka Y, Maejima K, Lawlor RT, Nakanishi Y, Mitsuhashi T, Fujimoto A, Furuta M, Ruzzenente A, Conci S, Oosawa A, Sasaki-Oku A, Nakano K, Tanaka H, Yamamoto Y, Michiaki K, Kawakami Y, Aikata H, Ueno M, Hayami S, Gotoh K, Ariizumi SI, Yamamoto M, Yamaue H, Chayama K, Miyano S, Getz G, Scarpa A, Hirano S, Nakamura T and Nakagawa H. Genomic characterization of biliary tract cancers identifies driver genes and predisposing mutations. J Hepatol 2018; 68: 959-969.

[17] Li M, Zhang Z, Li X, Ye J, Wu X, Tan Z, Liu C, Shen B, Wang XA, Wu W, Zhou D, Zhang D, Wang T, Liu B, Qu K, Ding Q, Weng H, Ding Q, Mu J, Shu Y, Bao R, Cao Y, Chen P, Liu T, Jiang L, Hu Y, Dong P, Gu J, Lu W, Shi W, Lu J, Gong W, Tang Z, Zhang Y, Wang X, Chin YE, Weng X, Zhang H, Tang W, Zheng Y, He L, Wang H, Liu Y and Liu Y. Whole-exome and targeted gene sequencing of gallbladder carcinoma identifies recurrent mutations in the ErbB pathway. Nat Genet 2014; 46: 872-876.

[18] Guan B, Wang TL and Shih Ie M. ARID1A, a factor that promotes formation of SWI/SNF-mediated chromatin remodeling, is a tumor suppressor in gynecologic cancers. Cancer Res 2011; 71: 6718-6727.

[19] Jin G, Ma H, Wu C, Dai J, Zhang R, Shi Y, Lu J, Miao X, Wang M, Zhou Y, Chen J, Li H, Pan S, Chu M, Lu F, Yu D, Jiang Y, Dong J, Hu L, Chen Y, Xu L, Shu Y, Pan S, Tan W, Zhou B, Lu D, Wu T, Zhang Z, Chen F, Wang X, Hu Z, Lin D and Shen H. Genetic variants at 6p21.1 and 7p15.3 are associated with risk of multiple cancers in Han Chinese. Am J Hum Genet 2012; 91: 928-934.

[20] Fidalgo F, Gomes EE, Moredo Facure L, Da Silva FC, Carraro DM, de Sa BC, Duprat Neto JP and Krepischi AC. Association of melanoma with intraepithelial neoplasia of the pancreas in three patients. Exp Mol Pathol 2014; 97: 144-147.

[21] Chen J, Somanath PR, Razorenova O, Chen WS, Hay N, Bornstein P and Byzova TV. Akt1 regulates pathological angiogenesis, vascular maturation and permeability in vivo. Nat Med 2005; 11: 1188-1196.

[22] Fehrenbacher N, Bar-Sagi D and Philips M. Ras/MAPK signaling from endomembranes. Mol Oncol 2009; 3: 297-307.

[23] Mondaca S, Nervi B, Pinto M and Abou-Alfa GK. Biliary tract cancer prognostic and predictive genomics. Chin Clin Oncol 2019; 8: 42.

[24] Lipkin SM, Wang V, Stoler DL, Anderson GR, Kirsch I, Hadley D, Lynch HT and Collins FS. Germline and somatic mutation analyses in the DNA mismatch repair gene MLH3: evidence for somatic mutation in colorectal cancers. Hum Mutat 2001; 17: 389-396.

[25] Baglietto L, Lindor NM, Dowty JG, White DM, Wagner A, Gomez Garcia EB, Vriends AH; Dutch Lynch Syndrome Study Group, Cartwright NR,

Barnetson RA, Farrington SM, Tenesa A, Hampel H, Buchanan D, Arnold S, Young J, Walsh MD, Jass J, Macrae F, Antill Y, Winship IM, Giles GG, Goldblatt J, Parry S, Suthers G, Leggett B, Butz M, Aronson M, Poynter JN, Baron JA, Le Marchand L, Haile R, Gallinger S, Hopper JL, Potter J, de la Chapelle A, Vasen HF, Dunlop MG, Thibodeau SN and Jenkins MA. Risks of Lynch syndrome cancers for MSH6 mutation carriers. J Natl Cancer Inst 2010; 102: 193-201.

[26] https://cancer.sanger.ac.uk/cosmic/signatures/SBS/.

[27] Yin Y, Stephen CW, Luciani MG and Fahraeus R. p53 stability and activity is regulated by MDM2-mediated induction of alternative p53 translation products. Nat Cell Biol 2002; 4: 462-467.

[28] Olivier M, Hollstein M and Hainaut P. TP53 mutations in human cancers: origins, consequences, and clinical use. Cold Spring Harb Perspect Biol 2010; 2: a001008.

[29] Prior IA, Lewis PD and Mattos C. A comprehensive survey of Ras mutations in cancer. Cancer Res 2012; 72: 2457-2467.

[30] Bailey MH, Tokheim C, Porta-Pardo E, Sengupta S, Bertrand D, Weerasinghe A, Colaprico A, Wendl MC, Kim J, Reardon B, Ng PK, Jeong KJ, Cao S, Wang Z, Gao J, Gao Q, Wang F, Liu EM, Mularoni L, Rubio-Perez C, Nagarajan N, Cortés-Ciriano I, Zhou DC, Liang WW, Hess JM, Yellapantula VD, Tamborero D, Gonzalez-Perez A, Suphavilai C, Ko JY, Khurana E, Park PJ, Van Allen EM, Liang H; MC3 Working Group; Cancer Genome Atlas Research Network, Lawrence MS, Godzik A, Lopez-Bigas N, Stuart J, Wheeler D, Getz G, Chen K, Lazar AJ, Mills GB, Karchin R and Ding L. Comprehensive characterization of cancer driver genes and mutations. Cell 2018; 174: 1034-1035.

[31] Horn H, Lawrence MS, Chouinard CR, Shrestha Y, Hu JX, Worstell E, Shea E, Ilic N, Kim E, Kamburov A, Kashani A, Hahn WC, Campbell JD, Boehm JS, Getz G and Lage K. NetSig: network-based discovery from cancer genomes. Nat Methods 2018; 15: 61-66.

[32] Canon J, Rex K, Saiki AY, Mohr C, Cooke K, Bagal D, Gaida K, Holt T, Knutson CG, Koppada N, Lanman BA, Werner J, Rapaport AS, San Miguel T, Ortiz R, Osgood T, Sun JR, Zhu X, McCarter JD, Volak LP, Houk BE, Fakih MG, O'Neil BH, Price TJ, Falchook GS, Desai J, Kuo J, Govindan R, Hong DS, Ouyang W, Henary H, Arvedson T, Cee VJ and Lipford JR. The clinical KRAS(G12C) inhibitor AMG 510 drives anti-tumour immunity. Nature 2019; 575: 217-223.

[33] Ou SI, Jänne PA, Leal TA, Rybkin II, Sabari JK, Barve MA, Bazhenova L, Johnson ML, Velastegui KL, Cilliers C, Christensen JG, Yan X, Chao RC and Papadopoulos KP. First-in-human phase I/IB dose-finding study of adagrasib (MRTX849) in patients with advanced KRAS(G12C) solid tumors (KRYSTAL-1). J Clin Oncol 2022; [Epub ahead of print].

[34] Shen J, Ju Z, Zhao W, Wang L, Peng Y, Ge Z, Nagel ZD, Zou J, Wang C, Kapoor P, Ma X, Ma D, Liang J, Song S, Liu J, Samson LD, Ajani JA, Li GM, Liang H, Shen X, Mills GB and Peng G. ARID1A deficiency promotes mutability and potentiates therapeutic antitumor immunity unleashed by immune checkpoint blockade. Nat Med 2018; 24: 556-562.

[35] Claesson-Welsh L and Welsh M. VEGFA and tumour angiogenesis. J Intern Med 2013; 273: 114-127.

[36] Shibuya M. Vascular endothelial growth factor (VEGF) and its receptor (VEGFR) signaling in angiogenesis: a crucial target for anti- and pro-angiogenic therapies. Genes Cancer 2011; 2: 1097-1105.

[37] Peng H, Zhang Q, Li J, Zhang N, Hua Y, Xu L, Deng Y, Lai J, Peng Z, Peng B, Chen M, Peng S and Kuang M. Apatinib inhibits VEGF signaling and promotes apoptosis in intrahepatic cholangiocarcinoma. Oncotarget 2016; 7: 17220-17229.

[38] Casimiro MC, Velasco-Velazquez M, Aguirre-Alvarado C and Pestell RG. Overview of cyclins D1 function in cancer and the CDK inhibitor landscape: past and present. Expert Opin Investig Drugs 2014; 23: 295-304.

[39] Graf F, Mosch B, Koehler L, Bergmann R, Wuest F and Pietzsch J. Cyclin-dependent kinase 4/6 (cdk4/6) inhibitors: perspectives in cancer therapy and imaging. Mini Rev Med Chem 2010; 10: 527-539.

[40] Song G, Li Y and Jiang G. Role of VEGF/VEGFR in the pathogenesis of leukemias and as treatment targets (Review). Oncol Rep 2012; 28: 1935-1944.

[41] Sha M, Jeong S, Chen XS, Tong Y, Cao J, Sun HY, Xia L, Xu N, Wang X, Han LZ, Xi ZF, Zhang JJ, Kong XN and Xia Q. Expression of VEGFR-3 in intrahepatic cholangiocarcinoma correlates with unfavorable prognosis through lymphangiogenesis. Int J Biol Sci 2018; 14: 1333-1342.

**Supplementary Table 1.** 620 gene list

| AKT1 | ALK | BRAF | DDR2 | EGFR | FGFR1 | ERBB2 | KRAS | MAP2K1 | MET |
|---|---|---|---|---|---|---|---|---|---|
| GAPDH | RPP30 | APC | TSC1 | TSC2 | CDK4 | CDKN2A | NF1 | NF2 | NTRK1 |
| MSH2 | MSH6 | PMS2 | EPCAM | POLD1 | POLE | CHEK2 | RAD50 | AR | ARAF |
| FGFR3 | FLT3 | GNA11 | GNAQ | HRAS | IDH1 | IDH2 | KDR | KIT | MAP2K2 |
| SMO | AXIN2 | BLM | BMPR1A | CDC73 | CDH1 | CDKN1B | CDKN1C | EXT1 | EXT2 |
| SDHA | SDHB | SDHC | SDHD | TMEM127 | WT1 | WRN | VHL | MDC1 | ATR |
| FANCL | FANCM | SLX4 | ERCC1 | ERCC2 | ERCC3 | ERCC4 | RAD1 | XPA | XPC |
| PMS1 | PCNA | RRM1 | RFC1 | CHEK1 | HDAC1 | HDAC2 | IFNGR1 | IFNGR2 | IRF1 |
| MUC17 | KMT2C | KMT2D | FAT1 | ATRX | NAV3 | PTPRT | SMARCA4 | MXRA5 | ANK3 |
| CTNNB1 | KDM6A | KEAP1 | EP300 | EPHA5 | EPHA3 | COL5A1 | MED12 | RBM10 | CIC |
| KMT2A | ERG | TSHZ3 | PIK3CG | ALPK2 | ARHGAP35 | STAG2 | BCLAF1 | NOTCH2 | NSD1 |
| TAF1 | TET1 | ASXL1 | SETBP1 | CUX1 | PAK7 | EPHB1 | CHD8 | USP9X | KDM5C |
| SOX9 | CDK12 | AMER1 | IRS2 | EPHA7 | TSHZ2 | ASXL2 | TP53BP1 | IKZF1 | KEL |
| TGFBR2 | EPHB6 | RECQL4 | SOX17 | ARID5B | CNBD1 | LATS2 | RUNX1 | RPTOR | CTCF |
| AXL | INSR | NFE2L2 | FOXP1 | SLC26A3 | EPPK1 | PLCG2 | PPP2R1A | TCF7L2 | INPPL1 |
| MAP3K13 | INPP4B | HNF1A | ERCC5 | GNPTAB | DDX3X | MAP4K3 | DIS3 | CSF1R | IL7R |
| PGR | FGFR4 | CBL | RPS6KA4 | FUBP1 | SMAD3 | TSHR | MORC4 | ETV6 | MST1R |
| PIK3C3 | MBD1 | TRAF7 | CUL4B | SLC1A3 | CUL3 | SNX25 | NCOA3 | EZH2 | RPL22 |
| IRF4 | AKT3 | RARA | BTK | TOP1 | ETV1 | MPO | PAX5 | TNFAIP3 | PRX |
| IPO7 | OTUD7A | WASF3 | U2AF1 | CSF3R | MYCN | SYK | CD1D | TBC1D12 | FOXO1 |
| RXRA | TPX2 | TRAF3 | MPL | NUP93 | ALOX12B | LCTL | MICALCL | TCP11L2 | TDRD10 |
| EZH1 | MEF2B | STAT5B | CRIPAK | MAPK8IP1 | RPL5 | RSBN1L | MITF | SH2B3 | HIST1H3B |
| AKT2 | PAK1 | RAD21 | SUZ12 | GNA13 | GUSB | RPS6KB2 | CBFB | BRE | DIAPH1 |
| RAD54L | TNFRSF14 | YAP1 | PIK3R3 | YES1 | E2F3 | SUFU | RAC1 | FAM166A | BIRC3 |
| SHQ1 | FAM46C | BCL2 | AURKA | ERRFI1 | AZGP1 | HLA-B | KLHL8 | TAP1 | NFKBIA |
| ZNF620 | CD79B | INHA | IGF2 | MYD88 | STAT5A | CCNE1 | EIF4A2 | C3orf70 | HIST1H4E |
| HIST1H2BD | EIF2S2 | STX2 | MAPK1 | MYCL | XIAP | CRLF2 | ICOSLG | VTCN1 | PPP6C |
| CD70 | FGFBP1 | STK19 | CDKN2C | ZRSR2 | CXCR4 | CALR | STK40 | SH2D1A | FAM175A |
| PCBP1 | APOL2 | HIST1H3G | PNRC1 | VEGFA | NKX3-1 | POU2AF1 | CDKN2B | HIST3H3 | H3F3A |
| HIST1H3D | RAB35 | RHEB | LMO1 | HIST1H3I | TACC3 | BCL10 | RPS2 | TNF | HIST1H3F |
| KIF5B | FOXQ1 | HIST1H3A | NAB2 | FIP1L1 | CENPA | ID3 | MST1 | CCDC6 | CDKN2B-AS1 |
| NRAS | PIK3CA | PTEN | RET | ROS1 | SMAD4 | ATM | BRCA1 | BRCA2 | TP53 |
| STK11 | BRIP1 | PALB2 | BARD1 | BAP1 | NBN | RAD51C | RAD51D | MRE11A | MLH1 |
| BCL2L11 | CCND1 | CCND2 | CCND3 | CDK6 | ERBB3 | ERBB4 | ESR1 | FBXW7 | FGFR2 |
| MDM2 | MTOR | NOTCH1 | NTRK2 | NTRK3 | PDGFRA | PIK3R1 | PTCH1 | PTPN11 | RAF1 |
| FH | FLCN | HOXB13 | MAX | MEN1 | MLH3 | MUTYH | PRKAR1A | RB1 | SDHAF2 |
| RAD9A | RAD17 | FANCA | FANCB | FANCC | FANCD2 | FANCE | FANCF | FANCG | FANCI |
| XRCC1 | PARP1 | RAD51B | RAD51 | XRCC2 | XRCC3 | XRCC4 | XRCC5 | XRCC6 | PRKDC |
| JAK1 | JAK2 | TYK2 | B2M | MDM4 | DNMT3A | TERT | FLG | ARID1A | XIRP2 |
| SETD2 | CREBBP | PTPRD | SACS | PBRM1 | ARID2 | GRIN2A | NOTCH3 | ZFHX3 | SPEN |
| NCOR1 | NOTCH4 | ARID1B | BCOR | LRRK2 | CHD4 | MGA | PTPRS | CARD11 | GATA3 |
| PIK3C2G | TMPRSS2 | POLQ | TBX3 | MAP3K1 | FLT1 | RNF43 | FLT4 | TET2 | COL5A3 |
| DOT1L | SF3B1 | FOXA1 | HGF | ANKRD11 | KMT2B | MYOCD | KDM5A | DICER1 | TLR4 |
| SOS1 | TP63 | IGF1R | GLI1 | SELP | RASA1 | JAK3 | LATS1 | NUP210L | BRD4 |
| SMC1A | MECOM | PDGFRB | SETDB1 | SLC4A5 | DNMT1 | IRS1 | DNER | GNAS | RICTOR |
| OR4A16 | AXIN1 | FRMD7 | SGK1 | ABL1 | SPOP | MAP2K4 | CASP8 | MED23 | PIK3CB |
| DNMT3B | LIFR | SMC3 | ZNF471 | TGFBR1 | EPHA2 | ITPKB | PIK3CD | DAXX | SMAD2 |
| INPP4A | INHBA | SIN3A | ADNP | ZRANB3 | RHOA | PARK2 | PRDM1 | DNAH12 | HSP90AB1 |
| ACVR1B | OR52N1 | RFWD2 | ACO1 | IRF6 | PIK3R2 | XPO1 | CDC27 | ZNF483 | PLK2 |
| CDKN1A | CNKSR1 | SERPINB13 | ZNF180 | ZNF750 | BCL6 | IKBKE | SMARCB1 | HIST1H1C | HIST1H1E |
| PPM1D | AJUBA | NFE2L3 | PHF6 | TBL1XR1 | CAP2 | MYB | NTN4 | MYC | CDK8 |
| TRIM23 | PDCD1 | KLF4 | GATA2 | TTLL9 | STAT3 | REL | HLA-A | NEGR1 | DDX5 |

| | | | | | | | | | |
|---|---|---|---|---|---|---|---|---|---|
| NKX2-1 | EIF1AX | ING1 | EWSR1 | GATA1 | FOXL2 | MYOD1 | CCDC120 | POU2F2 | SEPT12 |
| SOX2 | SRC | GSK3B | ELF3 | VEZF1 | ACVR2A | FGF3 | TCF3 | CEP76 | OMA1 |
| PHOX2B | MCL1 | MALT1 | JUN | BHMT2 | INTS12 | PAPD5 | PIM1 | FYN | EED |
| GPS2 | SMARCD1 | ACVR2B | GNB1 | ODAM | FOXA2 | IGF1 | RAD52 | QKI | SLC44A3 |
| ITGB7 | NBPF1 | H3F3C | ACVR1 | GOT1 | PDCD2L | TRAF2 | DNAJB1 | CTLA4 | RYBP |
| MAPK3 | EML4 | ATP5B | PDSS2 | RAB40A | SRSF2 | FGF19 | AURKB | CEBPA | SOCS1 |
| FGF4 | BBC3 | NPM1 | CD276 | IL10 | RIT1 | TIMM17A | CD274 | CD79A | EGR3 |
| GREM1 | EGFL7 | ALKBH6 | TXNDC8 | FLI1 | HIST1H3C | HIST1H3H | H3F3B | PDAP1 | SIRT4 |
| B4GALT3 | HIST1H3E | HIST1H3J | CRKL | EIF4E | CD74 | RPS15 | PDPK1 | BCL2L1 | DCUN1D1 |
| INSRR | STAT6 | TFE3 | PMAIP1 | PRKACA | HIST2H3D | SND1 | TCEB1 | BICC1 | EZR |

**Supplementary Table 2.** Germline gene list

| APC | ATM | AXIN2 | BAP1 | BARD1 | BLM | BMPR1A | BRCA1 | BRCA2 | BRIP1 |
|---|---|---|---|---|---|---|---|---|---|
| FH | FLCN | HOXB13 | MAX | MEN1 | MET | MLH1 | MLH3 | MRE11A | MSH2 |
| PRKAR1A | PTEN | RAD50 | RAD51C | RAD51D | RB1 | RET | SDHA | SDHAF2 | SDHB |
| CDC73 | CDH1 | CDK4 | CDKN1B | CDKN1C | CDKN2A | CHEK2 | EPCAM | EXT1 | EXT2 |
| MSH6 | MUTYH | NBN | NF1 | NF2 | NTRK1 | PALB2 | PMS2 | POLD1 | POLE |
| SDHC | SDHD | SMAD4 | STK11 | TMEM127 | TP53 | TSC1 | TSC2 | VHL | WRN |
| WT1 | | | | | | | | | |

**Supplementary Table 3.** Driver genes

| Symbol | ENSID | CGC | Chrom | Strand | Coordinates | MAX_ Coord | Width | N_ Mut | N_ Samples | Fra_ Uniq_ Samples | P |
|---|---|---|---|---|---|---|---|---|---|---|---|
| KRAS | ENSG00000133703 | TRUE | 12 | - | 2,539,828,425,398,280 | 25398284 | 2 | 10 | 10 | 1 | 0.0006 |
| IDH1 | ENSG00000138413 | TRUE | 2 | - | 209,113,113,209,113,000 | 209113113 | 1 | 2 | 2 | 1 | 0.0415 |

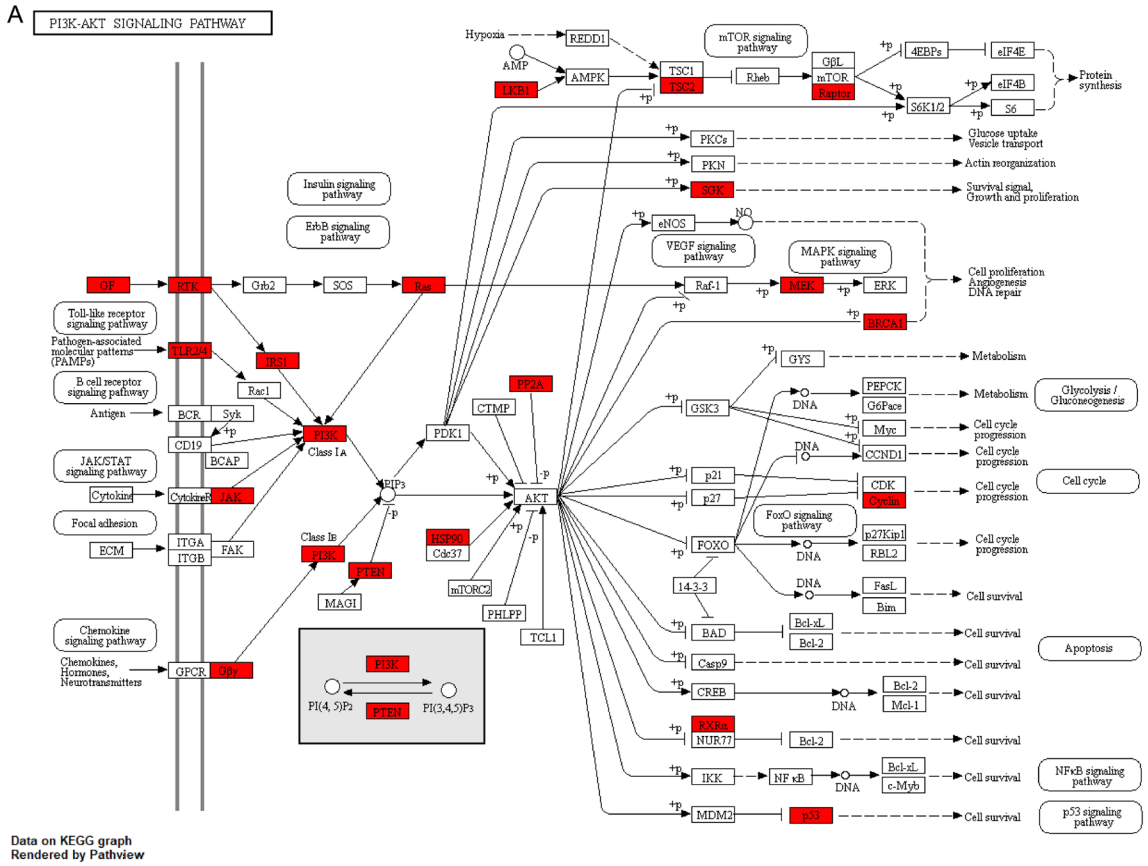
A
PI3K-AKT SIGNALING PATHWAY
Hypoxia
REDD1
AMP
LKB1
AMPK
TSC1
TSC2
mTOR signaling pathway
Rheb
GβL
mTOR
Raptor
4EBPs
eIF4E
eIF4B
S6K1/2
S6
Protein synthesis
PKCs
Glucose uptake
Vesicle transport
PKN
Actin reorganization
SGK
Survival signal,
Growth and proliferation
Insulin signaling pathway
ErbB signaling pathway
eNOS
NO
VEGF signaling pathway
MAPK signaling pathway
GF
RTK
Grb2
SOS
Ras
Raf-1
MEK
ERK
Cell proliferation
Angiogenesis
DNA repair
BRCA1
Toll-like receptor signaling pathway
Pathogen-associated molecular patterns (PAMPs)
TLR2/4
IRS1
B cell receptor signaling pathway
Antigen
BCR
Syk
Rac1
CD19
BCAP
PI3K
Class IA
PDK1
CTMP
PP2A
PIP3
AKT
JAK/STAT signaling pathway
Cytokine
CytokineR
JAK
Focal adhesion
ECM
ITGA
ITGB
FAK
Class IB
PI3K
PTEN
MAGI
HSP90
Cdc37
mTORC2
PHLPP
TCL1
Chemokine signaling pathway
Chemokines, Hormones, Neurotransmitters
GPCR
Gβγ
PI3K
PI(4, 5)P2
PTEN
PI(3,4,5)P3
GYS
Metabolism
GSK3
DNA
PEPCK
G6Pace
Glycolysis / Gluconeogenesis
Myc
CCND1
Cell cycle progression
p21
p27
CDK
Cyclin
Cell cycle
FoxO signaling pathway
FOXO
p27Kip1
RBL2
14-3-3
FasL
Bim
Cell survival
BAD
Bcl-xL
Bcl-2
Apoptosis
Casp9
CREB
Mcl-1
RXRα
NUR77
IKK
NF κB
c-Myb
NFκB signaling pathway
MDM2
p53
p53 signaling pathway
Data on KEGG graph
Rendered by Pathview

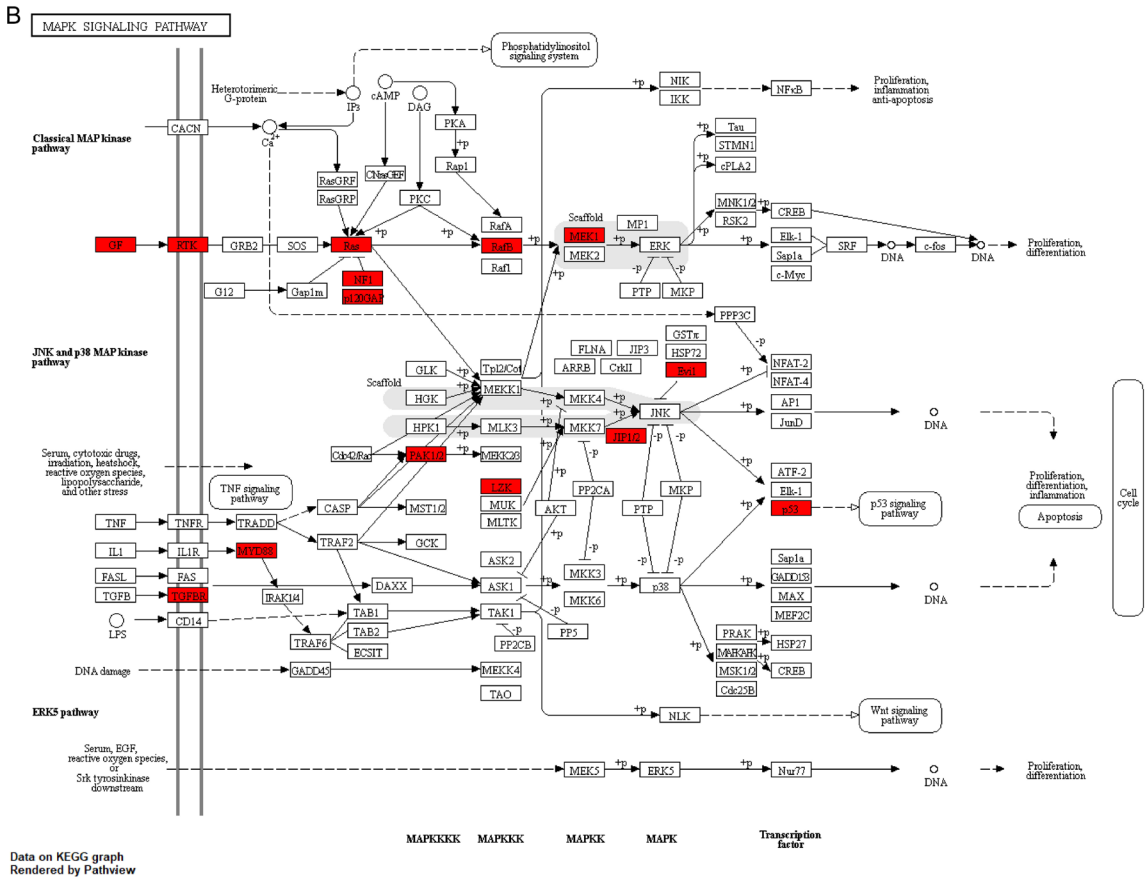
B
MAPK SIGNALING PATHWAY
Phosphatidylinositol signaling system
Heterotorimeric G-protein
IP3
cAMP
DAG
PKA
Rap1
NIK
IKK
NFκB
Proliferation, inflammation anti-apoptosis
Classical MAP kinase pathway
CACN
Ca2+
RasGRF
RasGRP
CNsGEF
PKC
Tau
STMN1
cPLA2
MNK1/2
RSK2
CREB
GF
RTK
GRB2
SOS
Ras
RafA
RafB
Raf1
Scaffold
MEK1
MEK2
MP1
ERK
Elk-1
Sap1a
c-Myc
SRF
c-fos
DNA
Proliferation, differentiation
G12
Gap1m
NF1
p120GAP
PTP
MKP
PPP3C
JNK and p38 MAP kinase pathway
GLK
HGK
HPK1
Tpl2/Cot
MEKK1
MLK3
MEKK2/3
Cdc42/Rac
PAK1/2
FLNA
ARRB
JIP3
CrkII
GSTπ
HSP72
Evi1
MKK4
MKK7
JNK
JIP1/2
NFAT-2
NFAT-4
AP1
JunD
ATF-2
Elk-1
p53
p53 signaling pathway
Proliferation, differentiation, inflammation
Apoptosis
Cell cycle
Serum, cytotoxic drugs, irradiation, heatshock, reactive oxygen species, lipopolysaccharide, and other stress
TNF signaling pathway
TNF
TNFR
TRADD
CASP
MST1/2
TRAF2
GCK
IL1
IL1R
MYD88
FASL
FAS
TGFB
TGFBR
IRAK1/4
DAXX
LZK
MUK
MLTK
ASK2
ASK1
TAK1
AKT
PP2CA
PP2CB
PP5
MKK3
MKK6
p38
Sap1a
GADD153
MAX
MEF2C
LPS
CD14
TAB1
TAB2
TRAF6
ECSIT
PRAK
MAPKAPK
HSP27
CREB
MSK1/2
Cdc25B
DNA damage
GADD45
MEKK4
TAO
ERK5 pathway
NLK
Wnt signaling pathway
Serum, EGF, reactive oxygen species, or Srk tyrosinkinase downstream
MEK5
ERK5
Nur77
Proliferation, differentiation
MAPKKKK
MAPKKK
MAPKK
MAPK
Transcription factor
Data on KEGG graph
Rendered by Pathview

**Supplementary Figure 1.** Mutated genes in the signaling pathway. A. Mutated genes (red box) of 59 BTC patients in the PI3K-AKT signaling pathway. B. Mutated genes (red box) of 59 BTC patients in the MAPK signaling pathway.

**Supplemental Table 4.** Actionable mutations

| Patient ID | Gene | Protein change |
|---|---|---|
| 1810011 | KRAS | p.G12V |
| 1810011 | CDKN2A | p.T95fs |
| 1810233 | KRAS | p.A146V |
| 1810276 | BRCA2 | p.E2175Q |
| 1810286 | U2AF1 | p.S34F |
| 1810433 | KRAS | p.G12S |
| 1810433 | BRCA2 | p.K3267N |
| 1810433 | HRAS | p.V14M |
| 1810433 | ATM | p.D661N |
| 1810455 | KRAS | p.G12D |
| 1810456 | ATM | p.Q1839X;p.H1847D |
| 1810558 | PIK3CA | p.E542K |
| 1810558 | KRAS | p.G12S |
| 1810595 | IDH2 | p.R172K |
| 1810709 | KRAS | p.G12C |
| 1810709 | MAP2K1 | p.C121S |
| 1830027 | IDH1 | p.R132C |
| 1830027 | PTEN | p.V255E |
| 1910134 | TSC2 | p.L717V |
| 1910201 | KRAS | p.G12D |
| 1910313 | MET | Amplification |
| 1910463 | BRCA2 | p.L1390fs |
| 1910611 | MAP2K1 | p.C121S |
| 1910783 | KRAS | p.G12D |
| 1910783 | CDKN2A | p.L31P |
| 1910937 | MET | Amplification |
| 1911157 | PIK3CA | p.H1047R |
| 1911364 | FGFR3 | p.E364K |
| 1911364 | BRAF | p.N581S |
| 1911369 | ALK | p.L93V |
| 1911369 | BRCA2 | p.L977F |
| 1911369 | IDH1 | p.L88F |
| 1911369 | CDKN2A | p.R98L |
| 1911369 | ATM | p.P884A |
| 1911369 | NF1 | p.I334M;p.S382F |
| 1911518 | MDM2 | Amplification |
| 1911551 | BRCA1 | p.M751L |
| 1911551 | KRAS | p.G12A |
| 1912208 | KRAS | p.G12C |
| 1912208 | RET | p.R313Q |
| 1912564 | TSC2 | p.L493I |
| 1912564 | BRCA2 | p.T3033fs |
| 1912564 | FGFR1 | p.R601W |
| 1912564 | CDKN2A | p.G23fs |

| | | |
|---|---|---|
| 1912568 | EGFR | Amplification |
| 1912569 | ERBB2 | p.S310Y |
| 1912694 | IDH1 | p.R132C |
| 1912695 | PTEN | p.R55fs |
| 1930033 | EGFR | Amplification |
| 1930033 | CDK4 | Amplification |
| 1930095 | BRCA1 | p.G1738del |
| 1930095 | KDM6A | p.Q710del |
| 1930095 | NF1 | p.S2687fs |
| 1930162 | KRAS | p.G12V |
| 1930179 | MDM2 | Amplification |
| 1930184 | BRAF | p.G469E |
| 1930629 | ATM | p.Y1957fs |